Low frequency recovery for ambient seismic data from ultra-dense linear arrays

Iga Pawelec and Paul Sava, Center for Wave Phenomena, Colorado School of Mines

SUMMARY

Although with the advent of wireless nodes seismic data are commonly acquired as continuous-time recordings, most of the information not related to active source effort is discarded. Ambient data are a valuable source of low frequency information, with the potential to enhance near-surface characterization using surface waves. We demonstrate that recovering meaningful low frequency signals from geophone arrays is possible down to about 10% of geophone's natural frequency if we remove near-DC thermal trends and suppress events causing instrument clipping. Interferometric processing allows us to compute phase velocity spectra with clear fundamental mode but since the dominant ambient energy direction is not always aligned with array, care must be taken when inverting for shear wave velocity profile.

We also reveal diurnal trends in instrument self-noise, with the strongest amplitudes located near DC component and weaker signals at 10 Hz and higher frequencies. Our analysis shows that temperature is an important driving factor of instrument self-noise, and that a dedicated noise suppression scheme could improve both active and ambient data quality.

INTRODUCTION

In land seismic acquisition, receivers are much smaller and easier to deploy than sources. Although efforts are made to create low-impact portable land sources (Châtenay, 2019), the real land acquisition revolution over the last two decades focused on receivers. Since early land wireless systems (Wilcox, 2015), land nodes have evolved, shrinking in size, providing longer battery life and reducing the seismic signal distortion (Dean et al., 2018). The shift from cabled to wireless acquisition is primarily motivated by the need for higher productivity and trace density in exploration seismology (Mougenot, 2004; Freed, 2008; Manning et al., 2018), however 3C land nodes are also an increasingly popular choice for short-time deployments in observational seismology (Ward and Lin, 2017; Wang et al., 2017). Two important consequences of introducing autonomous nodes are geometry design flexibility, that allows one to select the record length after rather than before data are acquired.

We focus our investigations on the commonly discarded portions of continuous recordings such as quiet times with no active sources to assess the ambient data potential to aid in active data processing. Specifically, we focus on recovering low frequencies and on interferometric processing to the create phase velocity spectra and invert for near surface shear wave profiles.

Our analysis is based on a field experiment acquired with a densely sampled linear array of 10 Hz nodes deployed for 5 days and recording continuously, including during active acquisition with a Vibroseis source. We show that nodes exhibit diurnal trends close to 0 Hz and at higher frequencies (10 and 12 Hz). This instrument response is likely driven by temperature changes, resulting in different levels and frequencies of instrument noise. We also present a processing flow for extracting low frequency surface wave velocity from ambient recording, complementing information obtained from active data. Dense sampling affords a unique opportunity to look at unaliased surface waves both in active data and in correlated ambient gathers. Ambient recordings enhance the resolution of phase velocity spectra at low frequencies, but linear arrays do not allow for correct estimation of the dominant direction of incoming energy. The resulting spectra have peaks at apparent velocities rather than actual velocities representing the site (Bozdağ and Kocaoğlu, 2005).

DATA AND PROCESSING

We use data acquired as a part of the Colorado School of Mines geophysical field camp to illustrate temperature-driven instrument noise, the unexpected effect of high-energy spike-like events on the computed spectra, and the processing flow which addresses these challenges to enhance low frequencies and recover meaningful phase velocity spectra. The data were acquired in Pagosa Springs, a geothermal area in south-west Colorado. A linear array of 392 blind nodes was deployed for 5 days, with a receiver spacing of 1.25 m with the objective of comparing nodal and cabled geophone arrays and evaluating the benefits of super fine sampling. Recording time included active seismic sources with Vibroseis non-linear upsweep between 4-140 Hz, as well as quiet night-time at a sparsely populated area (Figure 1).

Low frequency data are particularly valuable. Acoustic impedance inversion needs low frequencies to ensure the accuracy of the inverted values (Monk, 2020), while full waveform inversion benefits from low frequencies thanks to their ability to reduce cycle skipping, allowing for less accurate starting models (Virieux and Operto, 2009; Hu et al., 2018). Acquiring reliable low frequency data with Vibroseis can be challenging due to the mass displacement limit restricting the force output at low frequencies (Sallas, 2010). This challenge can be partially overcome with the employment of low-dwell sweeps (Tellier and Ollivrin, 2019), at increased survey duration and higher cost. However, thanks to continuous-time recording, important low frequency information could be supplemented by ambient noise processing. Using ambient noise to enhance active seismic experiments is not new. Halliday et al. (2008) discuss how sources encountered in suburban environment (e.g. cars) can be used in interferometric experiments to estimate and remove the groundroll (Halliday et al., 2007) or derive near surface velocity profiles (Roth and Holliger, 1999; Park et al., 1999). Ambient recordings with distributed acoustic sensing (DAS) also facilitate deriving shear wave velocity profiles and time-lapse velocity monitoring (Dou et al., 2017; Yuan et al., 2020;

Shragge et al., 2021), or help enhance active data imaging (Girard and Shragge, 2020b). However, geophones are not designed for low frequency operation: instrument sensitivity drops drastically below its natural frequency (usually a few Hz) and thermal response can dominate the low end of the spectrum. We discuss how to address these challenges in data processing and maximize the benefits of low frequencies in both active and ambient data.

Geophone impulse response

Geophones use a coil around a magnet which according to Faraday's Law of magnetic induction responds to the velocity of the proof mass (Hons and Stewart, 2006). When the measured frequencies match the natural frequency of the geophone, its output is nearly proportional to the ground particle velocity (Hons and Stewart, 2006). The ratio of geophone output voltage to the input ground motion is described by the geophone equation,

$$H(\omega) = G_0 \frac{\omega^2}{-\omega^2 + 2i\lambda\omega_0\omega + \omega_0^2}, \quad (1)$$

where G_0 is the geophone sensitivity expressed in V/m/s, ω_0 is the natural angular frequency, and λ is a dimensionless damping ratio. Equation 1 implies that amplitudes roll off below ω_0 and a phase shift is introduced to the low frequency portion of the data. Monk (2020) demonstrates the negative consequences of neglecting the instrument response correction on the coherence of low frequency data after spiking deconvolution. Since SNR at the low frequency end of the spectrum is often quite low, the noisy components can dominate phase estimation at such frequencies. Applying instrument response correction (e.g., by spectral division using equation 1) brings low frequencies closer to the level of high frequencies, thus limiting their impact on phase estimations and ensuring better phase coherence after deconvolution. Ambient data can have similarly small SNR at low frequencies, especially in the presence of strong near-surface heterogeneity. Thus, if the bandwidth of interest includes frequencies both above and below the geophone natural frequency, instrument response correction should be applied to reduce the effect of phase shift in the subsequent interferometric processing. Figure 2 shows the power spectrum computed from raw data spanning 5 days, and The spectrum is averaged with 20 bins per octave. The expected drop in power below 10 Hz can be observed for most receivers, but some maintain strong signal down to DC component. This behavior is due to several strong, spike-like signals generated by heavy vehicles or Vibroseis shaking next to a node. If such signal reaches amplitudes close to the geophone's maximum signal level, the entire derived spectrum is affected, and information from quiet limes of low signal levels is not represented accurately. Time editing of the affected traces is needed to avoid boosting outliers in the corrected traces. Furthermore, geophone correction can only be applied within a certain frequency range which for these data we determine to be about 1 Hz, below which the thermal response drives the spectrum.

Environment-related instrument noise

To get meaningful ambient data correlations, we need to ensure that the recorded signal is related to ambient sources and not

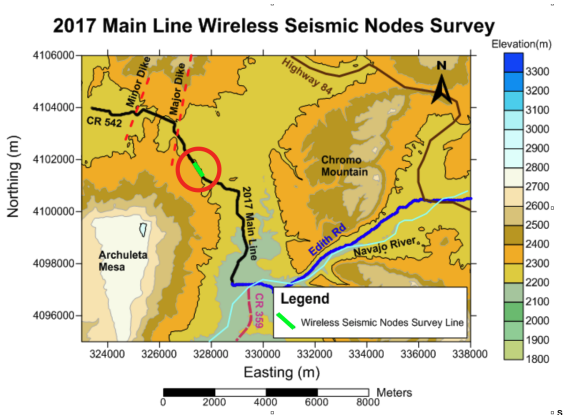

Figure 1: Approximate location of the nodal survey. Pagosa Springs is about 16 miles north-east of the wireless node line, and the location of temperature information in Figure 3 is the Stevens Field airport 18 miles north-east from the survey line.

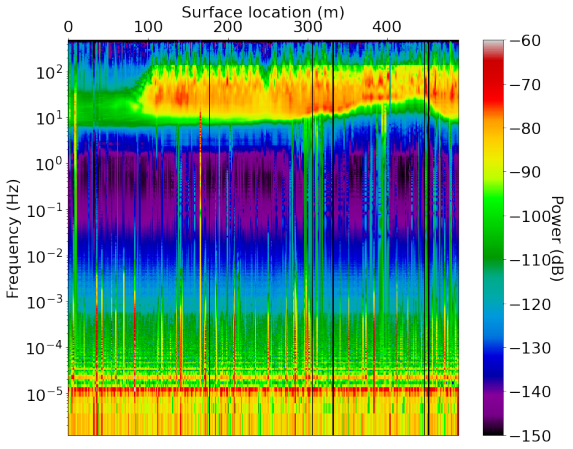

Figure 2: Power spectrum as a function of surface location. Note the significant drop in frequencies below 10 Hz except for several nodes that have anomalous behavior and appear to have strong energy almost to DC component.

to the instruments themselves. For DAS measurements, this consideration is not as prevalent since the measuring device is a continuous cable and thus the noise is not truly location-independent. Conversely, with blind nodes each sampling location provides an independent measuring point. This is a challenge since each node can be exposed to different soil conditions, ground coupling, and tilt. Consider the spectrograms in Figure 4 of 2 receivers offset by only 1.25 m. While the high-energy broadband events register similarly for both nodes, a strong diurnal trend centers at different frequencies (10 Hz and 12 Hz, respectively) and also appears more faintly at higher frequencies. The question arises: what is the origin of that signal? Since it appears consistently for closely-spaced nodes, it is not purely random, but given that its central frequency differs between the adjacent nodes at the same reference level, it is also unlikely to be a subsurface response. Similar observations were made for 3C Fairfield Nodal Zland

nodes in different acquisition settings: Johnson et al. (2019) report that ambient data recording is impacted by instrument noise modulated by temperature and wind conditions and related to the instrument coupling. Farrell et al. (2018) observe that an 11 kg weight on top of a node impacts the instrument noise band. Figure 3 shows the hourly temperature distribution recorded independently at the Stevens Field airport, about 18 miles north-east of the survey location. When compared to Figure 4, we can notice that high-temperature peaks coincide with top frequency in the trend of spectrograms, and thus temperature is possibly one of the driving factors for the instrumental noise.

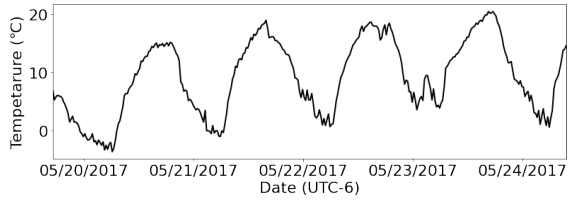

Figure 3: Hourly temperature variation during experiment. Note that daily temperature highs correspond to frequency increase for diurnal trends observed in Figure 4.

Ambient data processing

A workflow for ambient data processing to obtain surface wave phase velocity spectra is described by Bensen et al. (2007). The first step is to apply the instrument response correction, remove the thermal DC component and the low frequency trend (Figure 4). The usable bandwidth extends below 1 Hz, significantly lower than the instruments' natural frequency of 10 Hz, while the near-DC components are strongly attenuated. There is significant and persistent ambient signal in the bandwidth 2-6 Hz, similarly to the locally-generated seismic noise reported by Behm et al. (2014). To preserve this bandwidth, we bandpass and normalize the data in time using 1 s long running absolute mean, as proposed by Bensen et al. (2007). We split the data into 10 min windows for data recorded during quiet night-times (10 pm to 6 am) and use the RMS-based window rejection procedure suggested by Girard and Shragge (2020a) to eliminate windows with strong-energy events. Since some nodes in the array are noisy, we apply a median filter along the space axis to avoid the imbalance in the correlations. Finally, we form a virtual shot gather using cross-correlation and stacking technique, and compute the corresponding phase velocity spectrum (Figure 5(b)).

PHASE VELOCITY

Computing phase velocity spectra is the first step to deriving 1D shear wave velocity profiles by multichannel analysis of surface waves (MASW) (Park et al., 1999). MASW is used to create a high-resolution 2D shear wave profiles by interpolating adjacent 1D profiles Park et al. (2007). Although for reflection seismology surface waves are considered noise, they can provide valuable information about the near surface (Socco et al., 2010), and can be used to compute shear wave static corrections (Socco et al., 2015), delineate near surface shear wave velocity structure, or to model surface waves to subsequently subtract them from reflection records (Bai and Yilmaz, 2018).

We show the phase velocity spectra derived from an active Vibroseis shot (Figure 5(a)) and from the correlated interferometric gather (Figure 5(b)). Prior to deriving the spectra, we apply a geophone correction to boost the low frequencies and a mask to extract the surface wave content. The active data reveal a well-defined fundamental mode at 7-17 Hz, and what appears to be an interference of a higher mode at 17-40 Hz. One possible explanation of this phenomenon is the presence of stiff surface layer (Dal Moro, 2020). Below 7 Hz it is difficult to determine the shape of the dispersion curve, but phase velocities derived based on ambient data are well-defined for frequencies below 12 Hz. The fundamental mode between 4-8 Hz is much easier to pick on ambient data thanks to the presence of low frequencies and the selected 10 min correlation windows. However, the dispersion curve picked on ambient data indicates faster velocities than that picked for active data, which may be due to observing apparent velocities for out of plane incidence, rather than actual velocities for inline propagation (Bozdağ and Kocaoğlu, 2005).

CONCLUSION

We demonstrate that recovering meaningful low frequency signals from geophone arrays is possible down to about 10% of geophone's natural frequency provided that the near-DC thermal trends are removed and events causing instrument clipping are suppressed. Apart from the ultra-low frequency thermal trend, our data reveal higher frequency diurnal trends with different central frequencies that correlate well with the measured hourly temperature variations. This observation suggests that temperature is an important driving factor of instrument self-noise. If the noise overlaps with the bandwidth of interest, a dedicated noise suppression scheme improves both active and ambient data quality.

We also show that ambient data can provide access to low frequencies, which can be used to obtain surface wave phase velocity spectra with a well-defined fundamental mode. For linear arrays, the surface wave energy direction should align with the array in order to map data into real shear wave velocities instead of producing a directional projection. This obstacle can be overcome by applying a targeted window selection that only uses inline ambient sources, or with 2D arrays, that can handle broad wavefield directionality.

ACKNOWLEDGMENTS

We acknowledge Dawson and Sercel for providing equipment and technical support at the CSM Geophysical Field Camp, and GTI for facilitating dense sampling experiments with wireless nodes. We also acknowledge the CSM undergraduate students who conducted the acquisition, and SEG for providing partial financial support of our field acquisition. We extend our thanks to CWP sponsors for supporting this research.

ambient data processing

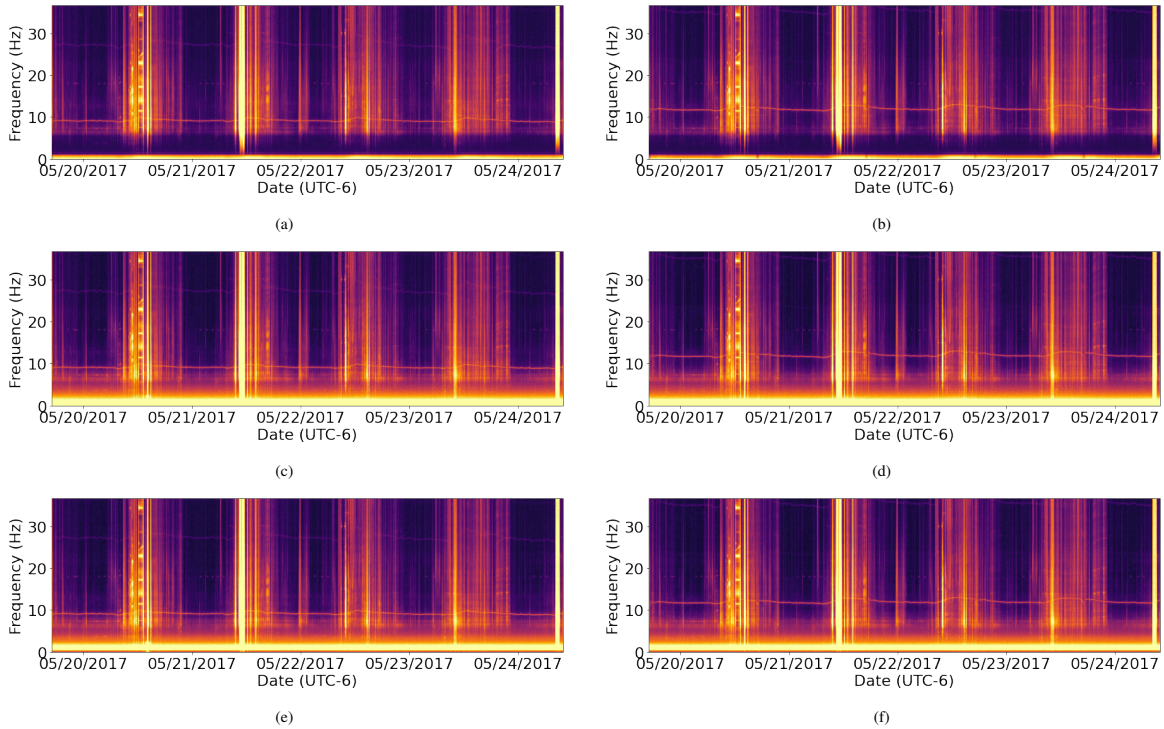

Figure 4: Spectrograms for two adjacent geophones separated by 1.25 m (left and right column, respectively). (a)-(b) are computed from raw data, (c)-(d) show the effect of the instrument response correction, and (e)-(f) have low-frequency trend removed. Note that despite the close proximity of the geophones, a strong diurnal trend appears at different frequencies.

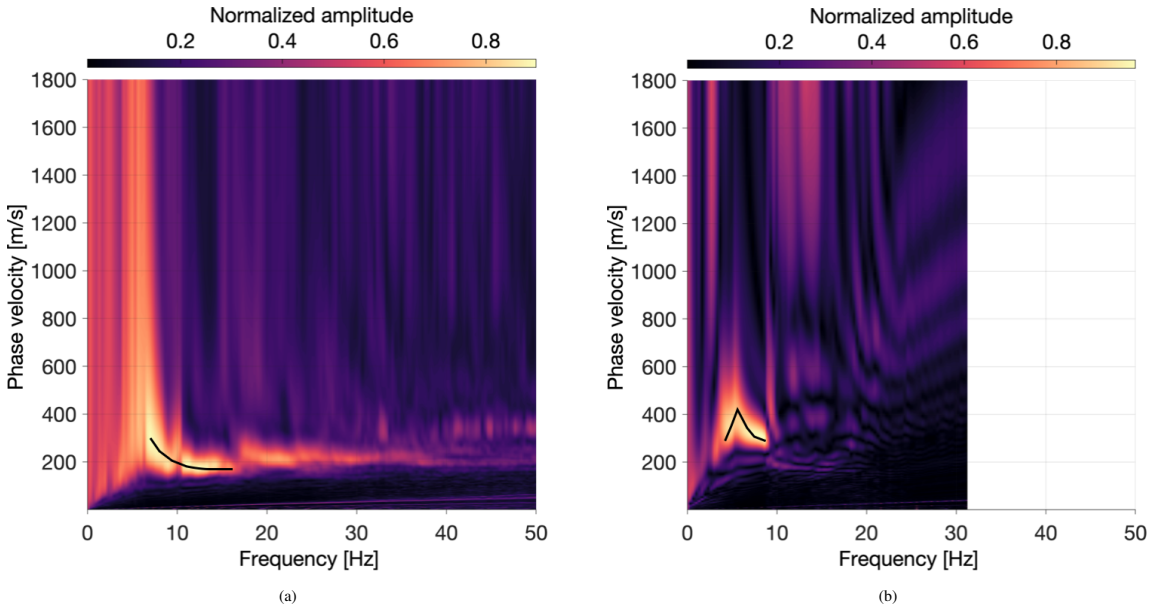

Figure 5: Phase velocity spectra with picked dispersion curves: (a) computed from an active shot after correlation and (b) computed from ambient data correlations. Note the different frequency range for the two plots. Ambient data have well defined spectra at 4-8 Hz - a range difficult to pick on the spectrum generated from an active shot.

REFERENCES

Bai, J., and O. Yilmaz, 2018, Model-based surface wave analysis and attenuation: 80th EAGE Conference and Exhibition 2018: Opportunities Presented by the Energy Transition, 1–5.

Behm, M., G. M. Leahy, and R. Snieder, 2014, Retrieval of local surface wave velocities from traffic noise - an example from the La Barge basin (Wyoming): Geophysical Prospecting, **62**, 223–243.

Bensen, G. D., M. H. Ritzwoller, M. P. Barmin, A. L. Levshin, F. Lin, M. P. Moschetti, N. M. Shapiro, and Y. Yang, 2007, Processing seismic ambient noise data to obtain reliable broad-band surface wave dispersion measurements: Geophysical Journal International, **169**, 1239–1260.

Bozdağ, E., and A. H. Kocaoğlu, 2005, Estimation of site amplifications from shear-wave velocity profiles in Yeşilyurt and Avcilar, Istanbul, by frequency-wavenumber analysis of microtremors: Journal of Seismology, **9**, 87–98.

Châtenay, A., 2019, Portable seismic survey device and method.

Dal Moro, G., 2020, The magnifying effect of a thin shallow stiff layer on Love waves as revealed by multi-component analysis of surface waves: Scientific Reports, **10**, 1–13.

Dean, T., J. Tulett, and R. Barnwell, 2018, Nodal land seismic acquisition: The next generation: First Break, **36**, 47–52.

Dou, S., N. Lindsey, A. M. Wagner, T. M. Daley, B. Freifeld, M. Robertson, J. Peterson, C. Ulrich, E. R. Martin, and J. B. Ajo-Franklin, 2017, Distributed Acoustic Sensing for Seismic Monitoring of the Near Surface: A Traffic-Noise Interferometry Case Study: Scientific Reports, **7**, 1–12.

Farrell, J., S. M. Wu, K. M. Ward, and F. C. Lin, 2018, Persistent noise signal in the FairfieldNodal three-component 5-Hz geophones: Seismological Research Letters, **89**, 1609–1617.

Freed, D., 2008, Cable-free nodes: The next generation land seismic system: The Leading Edge, **27**, 878–881.

Girard, A. J., and J. Shragge, 2020a, Automated processing strategies for ambient seismic data: Geophysical Prospecting, **68**, 293–312.

———, 2020b, Direct migration of ambient seismic data: Geophysical Prospecting, **68**, 270–292.

Halliday, D., A. Curtis, and E. Kragh, 2008, Seismic surface waves in a suburban environment: Active and passive interferometric methods: The Leading Edge, **27**, 210–218.

Halliday, D. F., A. Curtis, J. O. A. Robertsson, and D. J. van Manen, 2007, Interferometric surface-wave isolation and removal: Geophysics, **72**, A69–A73.

Hons, M., and R. Stewart, 2006, Transfer functions of geophones and accelerometers and their effects on frequency content and wavelets: CREWES Research Report, **18**, 1–18.

Hu, W., J. Chen, J. Liu, and A. Abubakar, 2018, Retrieving Low Wavenumber Information in FWI: An Overview of the Cycle-Skipping Phenomenon and Solutions: IEEE Signal Processing Magazine, **35**, 132–141.

Johnson, C. W., F. Vernon, N. Nakata, and Y. Ben-Zion, 2019, Atmospheric processes modulating noise in Fairfield nodal 5 Hz geophones: Seismological Research Letters, **90**, 1612–1618.

Manning, T., C. Brooks, A. Ourabah, M. Popham, D. Ablyazina, V. Zhuzhel, E. Holst, and N. Goujon, 2018, The case for a nimble node, towards a new land seismic receiver system with unlimited channels, *in* SEG Technical Program Expanded Abstracts 2018: Society of Exploration Geophysicists, 21–25.

Monk, D. J., 2020, Survey Design and Seismic Acquisition for Land, Marine, and In-between in Light of New Technology and Techniques: Society of Exploration Geophysicists.

Mougenot, D., 2004, Land seismic: Needs and answers: First Break, **22**, 59–63.

Park, C. B., R. D. Miller, and J. Xia, 1999, Multichannel analysis of surface waves: Geophysics, **64**, 800–808.

Park, C. B., R. D. Miller, J. Xia, and J. Ivanov, 2007, Multichannel analysis of surface waves (MASW)—active and passive methods: The Leading Edge, **26**, 60–64.

Roth, M., and K. Holliger, 1999, Inversion of source-generated noise in high-resolution seismic data: Leading Edge, **18**, 1402–1406.

Sallas, J. J., 2010, How do hydraulic vibrators work? A look inside the black box: Geophysical Prospecting, **58**, 3–18.

Shragge, J., J. Yang, N. Issa, M. Roelens, M. Dentith, and S. Schediwy, 2021, Low-frequency Ambient Distributed Acoustic Sensing (DAS): Case Study from Perth, Australia: Geophysical Journal International, **27708**, 1–19.

Socco, L. V., S. Foti, and D. Boiero, 2010, Surface-wave analysis for building near-surface velocity models—Established approaches and new perspectives: Geophysics, **75**, 75A83–75A102.

Socco, L. V., G. Mabyalaht, and C. Comina, 2015, Robust static estimation from surface wave data: SEG Technical Program Expanded Abstracts, **34**, 5222–5227.

Tellier, N., and G. Ollivrin, 2019, Low-frequency Vibroseis: Current achievements and the road ahead?: First Break, **37**, 49–54.

Virieux, J., and S. Operto, 2009, An overview of full-waveform inversion in exploration geophysics: Geophysics, **74**, WCC1–WCC26.

Wang, Y., F. C. Lin, B. Schmandt, and J. Farrell, 2017, Ambient noise tomography across Mount St. Helens using a dense seismic array: Journal of Geophysical Research: Solid Earth, **122**, 4492–4508.

Ward, K. M., and F. C. Lin, 2017, On the viability of using autonomous three-component nodal geophones to calculate teleseismic ps receiver functions with an application to old faithful, Yellowstone: Seismological Research Letters, **88**, 1268–1278.

Wilcox, S., 2015, Equipment QC approaches in land seismic acquisition: First Break, **33**, 95–100.

Yuan, S., A. Lellouch, B. Clapp, and B. Biondi, 2020, Near-surface seismic properties characterizations with a roadside distributed acoustic sensing (DAS) array: SEG Technical Program Expanded Abstracts 2020, Society of Exploration Geophysicists, 3457–3461.